Article ID: 1003－6326(2005)01－0200－07

Composite corrosion inhibitors for secondary alkaline zinc anodes①

JIA Zheng(贾 铮), ZHOU De-rui(周德瑞), ZHANG Cui-fen(张翠芬)
(Department of Applied Chemistry, Harbin Institute of Technology, Harbin 150001, China)

Abstract: The corrosion inhibition property of PEG600 and $In(OH)_3$ as composite corrosion inhibitors for secondary alkaline zinc electrodes was studied, and the inhibition efficiency was determined as 81.9%. The research focused on the mechanism by the methods of electrochemical impedance spectroscopy, polarization curves and IR spectroscopy. The results indicate that the corrosion inhibition effectiveness is attributed to the joint inhibition of anodic zinc dissolution and cathodic hydrogen evolution. And the anodic process is depressed to a greater extent than the cathodic process. The synergistic mechanism of the composite inhinbitors proves to be the enhancement of adsorption of PEG600 by $In(OH)_3$. Potentiostatic experiment results and SEM images verify the inhibition of dendritic growth by the composite inhibitors.

Key words: secondary alkaline zinc anode; composite corrosion inhibitors; corrosion inhibition; synergistic effect; dendritic growth

CLC number: TM 912.2 **Document code:** A

1 INTRODUCTION

Zinc, used as anode in many alkaline batteries like primary alkaline manganese, nickel-zinc, silver-zinc and zinc-air batteries, has been extensively investigated[1-3]. On the contrary, the zinc electrode in mercury-free rechargeable alkaline manganese batteries (RAM) has not drawn enough attention[4]. The main cause is that the reversibility of MnO_2 has been regarded as more crucial problem. However, recent researches[5, 6] indicated that the capacity fade of RAM was mainly caused by the gelled zinc anode which was designed to limit the capacity. Therefore, more emphases should be laid on the study of zinc anode in RAM. For RAM, a lot can be learned from other batteries in spite of the different configuration and characteristics of zinc electrodes.

The nonionic type surfactant with polyoxyethylene group is a potential corrosion inhibitor of alkaline zinc electrodes and recently the usage of it was actively researched. Nartey et al[7] identified PEG600 (polyethylene glycol 600) as a suitable organic inhibitor from eighteen organic compounds. Dobryszycki et al[8] confirmed the corrosion inhibition effectiveness of PEG400 along with Brij30 and FPEA too. Ein-Eli et al[9-11] conducted the electrochemical and surface investigations of zinc in alkaline solution containing such additives, and also verified that PEG600 is the most efficient inhibitor. An adsorption model of these additives was given to explain the superiority of PEG600. But their viewpoint that these additives inhibit corrosion by reducing cathodic hydrogen evolution process is suspicious because in their potentiodynamic measurements the cathodic process was actually composed of the process of zinc deposition and oxygen reduction besides hydrogen evolution. This is due to the presence of ZnO in KOH solutions and the presence of oxygen dissolved in the solutions. Therefore, the increased cathodic polarization induced by these additives doesn't necessarily mean the depression of corrosion.

Although these polyoxyethylene backbone based polymers have proven to be effective in respect of zinc corrosion-proof, they are not satisfactory compared with the better corrosion inhibition of mercury. The single addition of them is not enough to substitute mercury. In our previous works[12, 13], it was found that PEG600 had a synergistic effect with $In(OH)_3$ on inhibiting zinc corrosion, that is to say, the usage of both PEG600 and $In(OH)_3$ as composite inhibitors had better inhibition property than the individual usage of any one of these two inhibitors. Therefore, the further insight into the synergistic mechanism of the composite inhibitors is of theoretical and practical significance. In order to make clear the nature of mutual promotion of PEG600 and $In(OH)_3$, we performed a series of researches by electrochemical and spectroscopic methods. In addition to the corrosion inhibition property, other possible influences of composite inhibitors on cathodic deposition and anodic dissolution of zinc

① **Received date:** 2004－06－08; **Accepted date:** 2004－11－15
Correspondence: JIA Zheng; Tel: +86-451-55615972; E-mail: jiazjiazjz@yahoo.com.cn

were also evaluated.

2 EXPERIMENTAL

2.1 Electrochemical impedance spectroscopy (EIS) and steady-state polarization curve measurement

The working electrode was a well polished zinc (with purity of 99.995%) disk electrode. A large area sintered cadmium electrode served as counter electrode, and a Hg/HgO electrode as reference electrode. A 10 mol/L KOH solution was used as blank electrolyte. The sample electrolytes were 10 mol/L KOH solutions containing 10^{-3} mol/L PEG600 and/or 10^{-4} mol/L $In(OH)_3$. Before each experiment was started, the electrolyte was purged of oxygen with nitrogen for 30 min.

The equipment was a CHI660A electrochemical station (CH Instruments, Inc., Austin, USA). The electrochemical impedance spectra (EIS) of the electrode systems with different electrolytes were measured at different potentials. The amplitude of the disturbing sinusoidal wave was 5 mV.

The steady-state polarization curves were obtained by potentiodynamic method. The electrode potential swept from − 1.65 to − 1.05 V at a rate of 0.2 mV/s.

2.2 Infrared spectroscopy study

Two mirror polished zinc sheets were respectively immersed in a 9 mol/L KOH solution containing 0.1% PEG600 and a 9 mol/L KOH solution containing 0.1% PEG600 and 0.1% $In(OH)_3$ for 12 h. After the two sheets were taken out, they were washed with distilled water and wiped with absorbent cotton with ethanol. Then the infrared spectroscopy (Equinox type, Bruker, German) data were obtained from the two zinc sheets.

2.3 Potentiostatic step measurement and scanning electron microscopy (SEM)

Zinc disk electrodes were immersed in 9 mol/L KOH electrolytes (with 70 g/L ZnO) containing different additives. When the potential was controlled at 150 mV negative to open-circuit potential (OCP), the corresponding $I-t$ curves were recorded. Then, the zinc electrodes were dragged out, and the deposit on the electrode was carefully scraped off. After the deposit was washed with distilled water and dried, the morphology of them was observed by SEM.

3 RESULTS AND DISCUSSION

3.1 Influences of composite inhibitors on cathodic hydrogen evolution and anodic zinc dissolution of zinc electrodes

Fig. 1 shows the Nyquist plots for the zinc electrodes measured at different potentials. For comparison, the plots obtained from the blank electrolyte and the sample electrolyte are depicted in the same graphs.

In each EIS Nyquist plot, the capacitive arc in the high frequency range can be considered as the response caused by the relaxation process of double-layer capacitance and charge-transfer resistance. And the capacitive arc can be simulated by the equivalent circuit in Fig. 2. The R_S in the circuit represents the solution resistance of the electrode system, and the R_{CT} represents the charge-transfer resistance (i.e., electrochemical reaction resistance), and the Q_{dl} is a constant phase element (CPE) describing the interface double-layer.

The parameters of the elements in the equivalent circuit were derived from the simulation of the corresponding complex impedance data by means of the software "EQUIVCRT", as listed in Table 1.

Table 1 Parameters of elements in equivalent circuits simulating capacitive arcs in high frequency range

Overpotential/mV	Additive	R_S/Ω	R_{CT}/Ω	Q_{dl}	
				Y_0/($s^n \cdot \Omega^{-1}$)	n
− 50	No	0.808 8	127.7	495.6	0.75
	Yes	1.077	151.5	30.63	0.91
0	No	1.256	7.761	79.92	0.96
	Yes	1.102	152.3	23.38	0.92
50	No	0.469 4	2.439	812.1	0.70
	Yes	1.312	60.47	24.19	0.95
100	No	1.304	0.623 6	1 142	0.81
	Yes	1.349	0.995 1	48.15	1.00

The influences of the composite inhibitors on the reaction rate under different polarization conditions can be directly observed by comparing the diameter of the capacitive arc, the charge transfer resistance (R_{CT}). It is defined as

$$K = R_{CT,\ sample}/R_{CT,\ blank}$$

where K is the increased times of R_{CT} caused by the composite inhibitors.

At $\eta = -50$ mV, the cathodic process occurring on the zinc is hydrogen evolution, not zinc deposition or oxygen reduction because of the absence of ZnO and O_2 in the electrolytes. That K is 1.19 means that the addition of the composite inhibitors slightly depresses the hydrogen evolution process. At the open circuit potential ($\eta = 0$ mV), K is 19.62, which indicates that the corrosion rate is significantly reduced with the presence of the

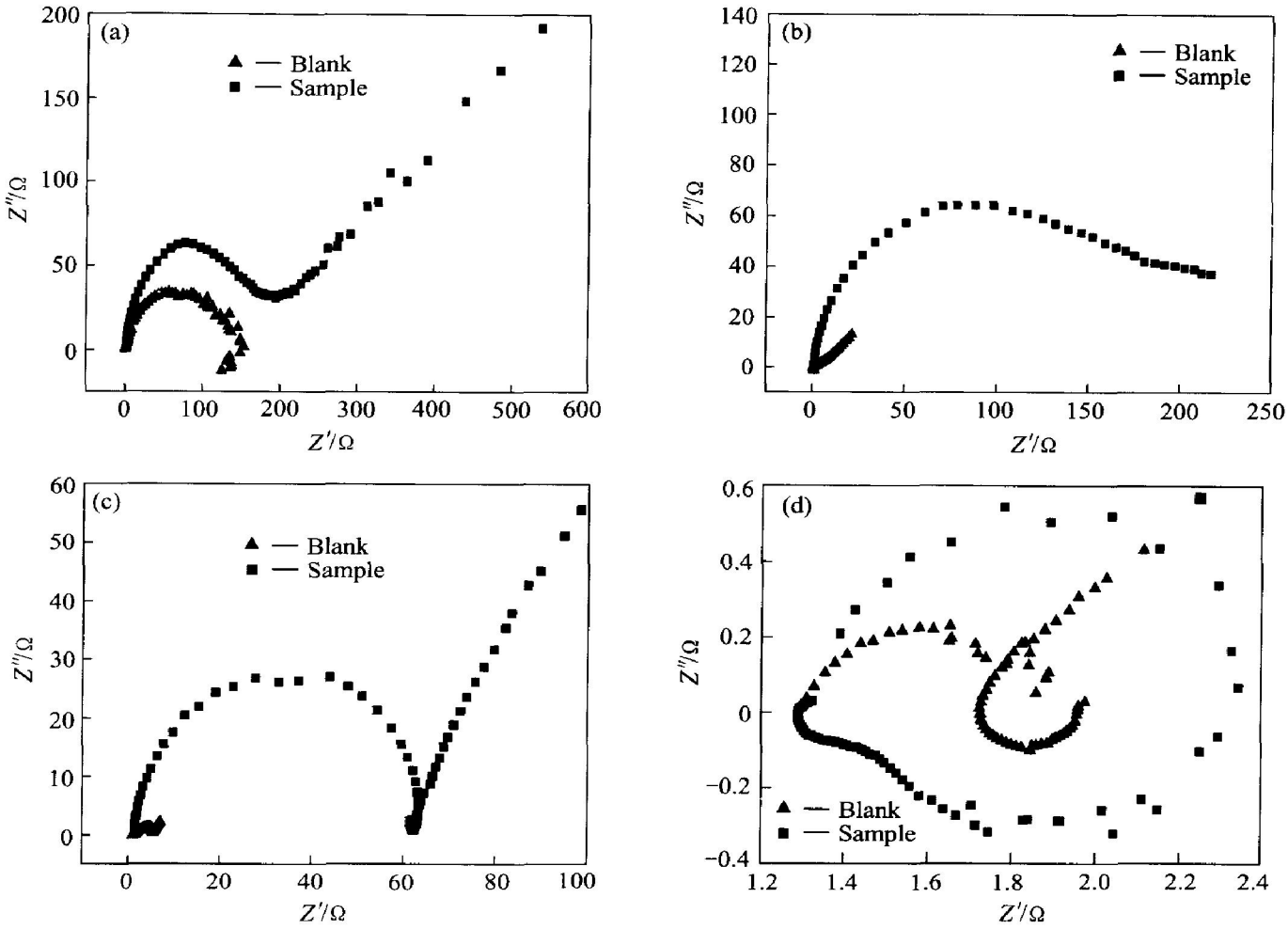

Fig. 1 Nyquist plots for zinc electrodes in 10 mol/L KOH solutions with no additive (Blank) and with 10^{-3} mol/L PEG600 and 10^{-4} mol/L $In(OH)_3$ (Sample) at η = − 50 mV(a), 0 mV(b), 50 mV(c), and 100 mV(d)

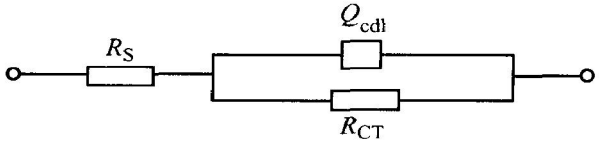

Fig. 2 Equivalent circuit of capacitive arc in high frequency range on Nyquist plots

composite inhibitors. At η = 50 mV, because the anodic zinc dissolution process is considerably inhibited, K is as high as 24.79. When the zinc is further polarized to η = 100 mV, the inhibition effect on zinc dissolution rapidly decreases, so K is reduced to 1.60. It can be inferred from the above analyses that the inhibition affects on both conjugated corrosion reactions, hydrogen evolution and zinc dissolution, and reduces the corrosion rate.

When a zinc-based battery using the composite inhibitors is in storage, the corrosion of zinc will be inhibited. When it is discharged, the inhibition effect on anodic zinc dissolution at high anodic overpotentials will decrease greatly so that an acceptable discharge performance can be achieved.

Fig. 3 presents the steady-state polarization curves of zinc electrodes with different additives. The electrochemical parameters of zinc are derived from these polarization curves through Tafel plot extrapolation as listed in Table 2.

It can be seen from Fig. 3 that the addition of $In(OH)_3$ only depresses the cathodic process, not the anodic one and causes a negative shift of the corrosion potential (φ_{corr}). This effect can be observed from Table 2 more clearly because cathodic Tafel slope (b_c) increases obviously while anodic Tafel stope (b_a) basically keeps invariable. According to Ref. [14], the change of corrosion potential $\Delta\varphi_{corr} = \frac{b_a b_c}{b_a + b_c} \lg\left[\frac{f_c}{f_a}\right]_{\varphi_{corr}}$, so the negative shift of φ_{corr} indicates that the effect coefficient on cathodic process f_c is smaller than that on anodic process f_a, that is to say, the cathodic process is depressed to a greater extent than the anodic process. In a word, $In(OH)_3$, as a cathode-type inhibitor, prevents corrosion mainly through slow-

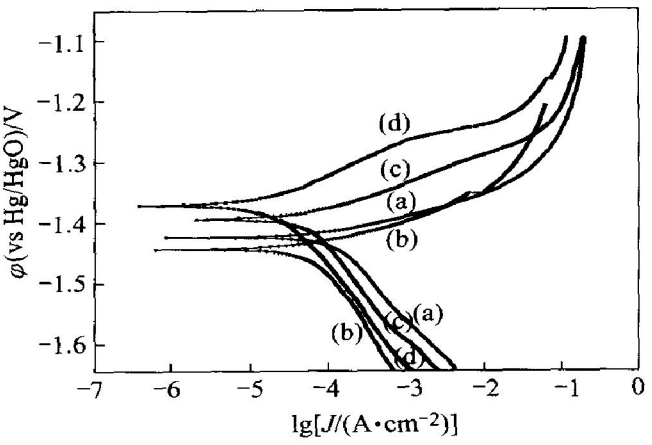

Fig. 3 Steady-state polarization curves of zinc electrodes in 10 mol/L KOH solutions with no additive(a), 10^{-4} mol/L In(OH)$_3$(b), 10^{-3} mol/L PEG600(c) and 10^{-3} mol/L PEG600+ 10^{-4} mol/L In(OH)$_3$(d)

Table 2 Electrochemical parameters of zinc derived from polarization curves in Fig. 2

Additive	φ_{corr}/mV	J_{corr}/(A·cm^{-2})	b_a/(mV·d^{-1})	b_c/(mV·d^{-1})	E_i/%
No	-1.424	1.09×10^{-4}	33.6	132.6	
In(OH)$_3$	-1.444	5.19×10^{-5}	32.5	193.2	52.2
PEG600	-1.395	6.01×10^{-5}	43.9	175.3	44.7
In(OH)$_3$+PEG600	-1.371	1.97×10^{-5}	57.2	162.2	81.9

ing down hydrogen evolution.

The shape and features of the polarization curve for the composite inhibitors are very similar to those for PEG600 indicating that they have the similar mechanism. The addition remarkably depresses both anodic and cathodic processes and causes a positive shift of φ_{corr}. It means that the anodic process is depressed to a greater extent than the cathodic process. Furthermore, the anodic branch of the polarization curves is noted to consist of three sections. The first section with higher slope than that obtained in the blank electrolyte corresponds to adsorption region, with the depression of the anodic process. In the next section, the slope of the curve decreases markedly with a rapid increase in anodic current. This corresponds to desorption region. In the last section, the trend of the curve almost approaches that obtained in the blank electrolyte. This can be called the blank region. With PEG600 molecules mainly desorbed, here the polarization behavior of zinc resembles that seen in the blank electrolyte. All these are in accordance with the results from EIS experiment.

Referring to Table 2, the differences between these two systems lie in the fact that the composite inhibitors have more obvious depression on anodic and cathodic reaction, and thus lowering corrosion current, and causing more positive shift of corrosion potential than PEG600. This indicates that PEG600 and In(OH)$_3$ have a synergistic effect on suppressing corrosion, which operates in the same way as PEG600.

In sum, in the case of the composite inhibitors, the polarization curve does not display any characteristic of that for In(OH)$_3$, but evidently follows the principle observed from that for PEG600 except that the depression effect on corrosion, especially on zinc dissolution, is strengthened. This phenomenon may be explained by the hypothesis that the absorption of PEG600 is enhanced by adding In(OH)$_3$. When In(OH)$_3$ is added into electrolyte, it will be immediately reduced into indium metal by zinc, and indium will cover the surface of zinc electrode. As we know, the electron configuration of zinc is [Ar] $4s^2$ $3d^{10}$, and the outer subshell is fully filled. On the contrary, the electron configuration of the indium is [Kr] $5s^2$ $4d^{10}$ $5p^1$, and there are vacant 5p subshells to accommodate the unshared pairs of electrons of oxygen atoms in PEG600. Therefore, the adsorption of PEG600 on indium surface seems energetically more favorable than that on zinc surface. In this way, the addition of In(OH)$_3$ helps the adsorption of PEG600 on zinc electrode surface.

3.2 Spectroscopic evidences for synergistic mechanism of composite inhibitors

Fig. 4 presents the IR spectra obtained from zinc immersed in alkaline electrolytes with PEG600 (spectrum b) and with the composite inhibitors (spectrum c). The spectrum of neat PEG600 (spectrum a) is presented for comparison. It is found that the characteristic spectrum bands of PEG600 are detected on both the treated zinc sheets indicating that PEG600 is definitely adsorbed on the zinc surface. In addition, the characteristic bands of PEG600 appearing in spectrum (c) is more distinct than those in spectrum (b), implying that more PEG600 molecules are adsorbed on zinc with indium coating produced from reduction of In(OH)$_3$ than on pure zinc.

The very broad and strong peak at 3 660-3 100 cm^{-1} in spectrum (a) is assigned to the stretch vibration of hydroxyl group coordinated between molecules by hydrogen bond[15]. And that this peak can be distinguished in spectra (b) and (c) indicates that the adsorbed PEG600 still has the terminating hydroxyl group.

The peak attributed to $\nu(CH_2)$ in spectrum (a) appears at 2 871 cm^{-1}, while this peak in spectra (b) and (c) appears respectively at 2 869 and 2 854 cm^{-1}. That is, the IR peak moves towards

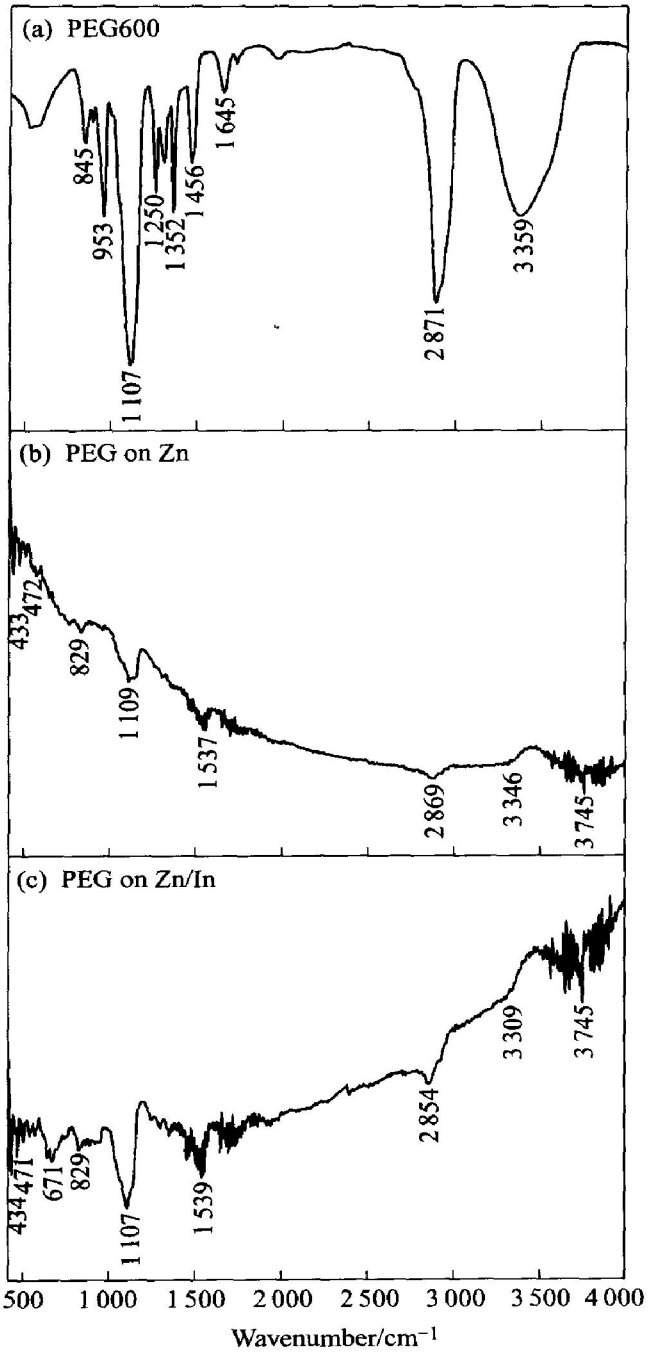

Fig. 4 IR spectra of neat PEG600(a) and zinc immersed in 9 mol/L KOH solution containing 0.1% PEG600(b) and 9 mol/L KOH solution containing 0.1% PEG600 and 0.1% $In(OH)_3$(c)

low frequency direction. The reason is that the position of the peak is affected by the adsorption interaction, i.e., the complexation between oxygen atom in PEG600 and metal on the zinc substrate. The stronger the interaction is, the larger the movement is. Therefore, it can be inferred that the adsorption of PEG600 is enhanced by the presence of $In(OH)_3$.

The strong peak at 1 107 cm^{-1} is the characteristic peak of stretch vibration of $-CH_2-O-CH_2-(\upsilon_{C-O})$. The relative intensity of this peak is different in these three spectra. The ratio of absorbance of υ_{C-O} to absorbance of $\upsilon(CH_2)$ in spectra (a), (b) and (c) is respectively 1.50, 3.29 and 4.26. This means that the stretch vibration of C—O in the molecule of adsorbed PEG600 is strengthened. This is due to the influence of the complexation between oxygen atom in PEG600 and metal on the zinc substrate. The highest ratio in spectrum (c) indicates that the existence of $In(OH)_3$ promotes the complexation, i.e., the adsorption of PEG600.

The peaks at 472 and 433 cm^{-1} appearing in spectra (b) and (c) are possibly attributed to the vibration of the coordination bond of zinc and oxygen in PEG600. And the peak at 671 cm^{-1} in spectrum (c) may be attributed to vibration of the coordination bond of indium and oxygen in PEG600. All these IR spectroscopic data provide good evidence for the above proposed synergistic mechanism of the composite inhibitors and can well interpret the results in polarization curves.

3.3 Influence of composite inhibitors on cathodic zinc deposition process of zinc electrode

Since high concentration of ZnO was dissolved in the alkaline electrolytes and the exchange current density of zinc deposition reaction is by far greater than that of hydrogen evolution on zinc, the zinc deposition process was almost the only one which proceeded in the potentiostatic cathodic polarization experiments. Therefore, the obtained $I-t$ curves depicted in Fig. 5 corresponds to the rate of zinc deposition and can be used to determine the influence of additives on zinc deposition process.

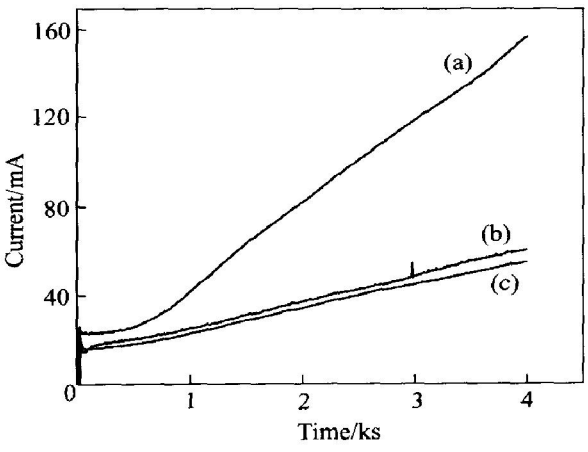

Fig. 5 $I-t$ curves of zinc at constant overpotential of −150 mV in 9 mol/L KOH electrolyte (with 70 g/L ZnO)(a), 9 mol/L KOH electrolyte (with 70 g/L ZnO) containing 10^{-3} mol/L PEG600(b), 9 mol/L KOH electrolyte (with 70 g/L ZnO) containing 10^{-3} mol/L PEG600+ 10^{-4} mol/L $In(OH)_3$(c)

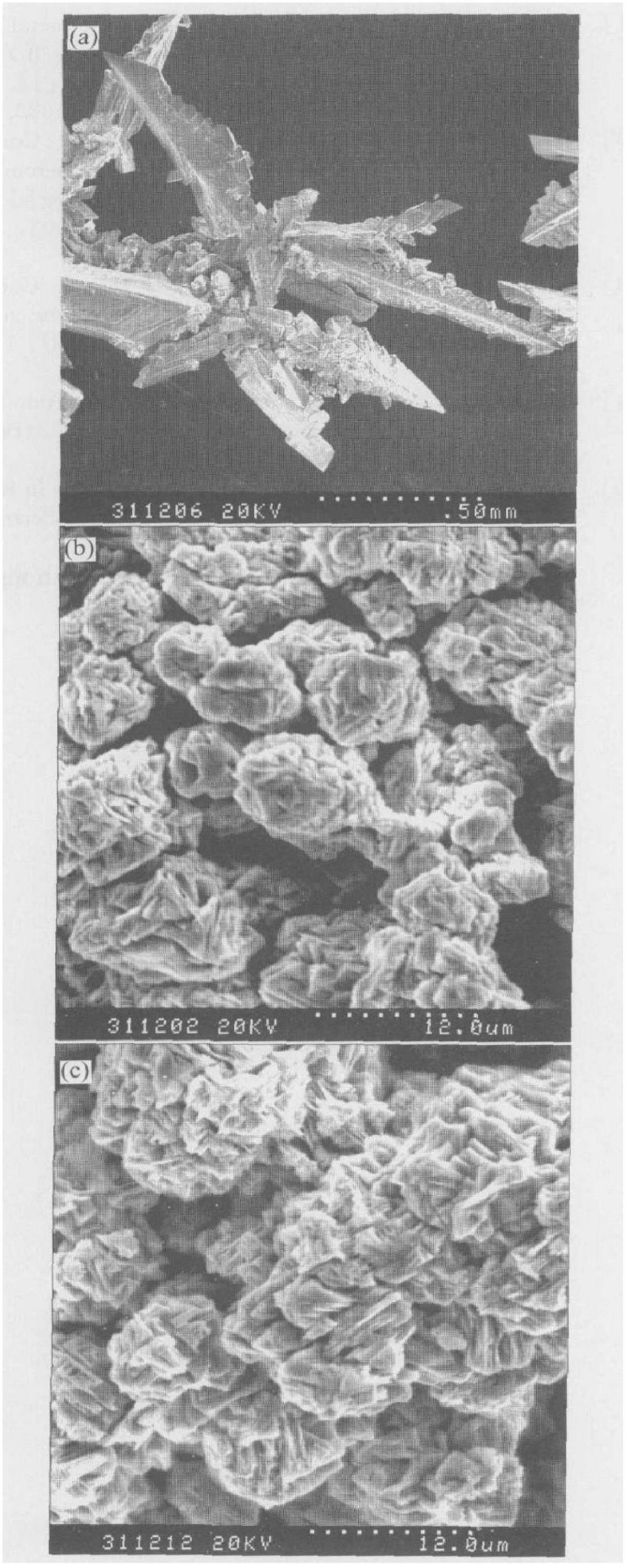

Fig. 6 SEM photographs of zinc deposit produced on electrode in 9 mol/L KOH electrolyte (with 70 g/L ZnO)(a), 9 mol/L KOH electrolyte (with 70 g/L ZnO) containing 10^{-3} mol/L PEG600(b), 9 mol/L KOH electrolyte (with 70 g/L ZnO) containing 10^{-3} mol/L PEG600+ 10^{-4} mol/L $In(OH)_3$(c)

It can be seen from Fig. 5 that the zinc deposition current first drops slightly and then increases on a large scale in the case of blank alkaline electrolyte (curve a). The rise in current in the potentiostatic experiments must be caused by the increase in true electrode surface area due to the formation of large-area deposit, which is most possibly zinc dendrite. And this is verified by the SEM photograph (a) shown in Fig. 6. The deposits are some needle-like zinc dendrites with predetermined orientations.

In the case of PEG600 and the composite inhibitors, the magnitude of current increment is largely reduced, implying that dendritic growth is avoided. The reason is that the adsorption of PEG600 inhibits the preferential growth of some certain crystal face and makes the deposition more uniform. By comparing curves (b) and (c) in Fig. 5, it can be found that this effect is somewhat greater with the composite inhibitors than just with PEG600. And this is owing to the enhancement of adsorption of PEG600 by $In(OH)_3$. It can be seen from Fig. 6(b) that PEG600 brought about isolated sphere-like granules. While the addition of the composite inhibitors produced more continuous, uniform deposits consisting of small crystallites (Fig. 6(c)).

4 CONCLUSIONS

1) EIS results and polarization curves show that the composite inhibitors have a good corrosion inhibition property for zinc with an inhibition efficiency of 81.9%, and that the mechanism is the joint inhibition of anodic zinc dissolution and cathodic hydrogen evolution.

2) Polarization curves and IR spectroscopic results demonstrate that the synergistic mechanism of the composite inhibitors is the enhancement of adsorption of PEG600 by indium coating reduced from $In(OH)_3$.

3) Cathodic zinc deposition process is modified by the composite inhibitors so that the formation of zinc dendrite is avoided.

REFERENCES

[1] Huot J Y, Malservisi M. High-rate capability of zinc anodes in alkaline primary cells[J]. J Power Sources, 2001, 96: 133-139.

[2] Chang H, Lim C. Zinc deposition during charging nickel/zinc batteries[J]. J Power Sources, 1997, 66: 115-119.

[3] Skelton J, Serenyi R. Improved silver/zinc secondary cells for underwater applications[J]. J Power Sources, 1997, 65: 39-45.

[4] Sharma Y, Aziz M, Yusof J, et al. Triethanolamine as an additive to the anode to improve the recharge-

ability of alkaline manganese dioxide batteries[J]. J Power Sources, 2001, 94: 129-131.

[5] SHEN Yu-wei, Kordesch K. The mechanism of capacity fade of rechargeable alkaline manganese dioxide zinc cells[J]. J Power Sources, 2000, 87: 162-166.

[6] JIA Zheng, ZHANG Cui-fen, ZHOU De-rui. Analysis of causes of capacity decline of rechargeable alkaline manganese battery during cycling[J]. Material Science & Technology, 2004, 12(2): 179-182.

[7] Nartey V K, Binder L, Kordesch K. Identification of organic corrosion inhibitors suitable for use in rechargeable alkaline zinc batteries[J]. J Power Sources, 1994, 52: 217-222.

[8] Dobryszycki J, Biallozor S. On some organic inhibitors of zinc corrosion in alkaline media[J]. Corrosion Science, 2001, 43: 1309-1319.

[9] Eir-Eli Y, Auinat M, Starosvetsky D. Electrochemical and surface studies of zinc in alkaline solutions containing organic corrosion inhibitors[J]. J Power Sources, 2003, 114: 330-337.

[10] Eir-Eli Y, Auinat M. The behavior of zinc metal in alkaline solution containing organic inhibitors(Ⅰ)—Electrochemical studies of zinc[J]. J Electrochem Soc, 2003, 150(12): A1606-A1613.

[11] Eir-Eli Y, Auinat M. The behavior of zinc metal in alkaline solution containing organic inhibitors(Ⅱ)—Identification of surface films formed on zinc[J]. J Electrochem Soc, 2003, 150(12): A1614-A1622.

[12] JIA Zheng, ZHOU De-rui, ZHANG Cui-fen. Composite additives to negative electrodes for mercury-free rechargeable alkaline manganese batteries[J]. Journal of Harbin Institute of Technology, 2003, 35(11): 1344-1346.

[13] JIA Zheng, ZHANG Cui-fen, ZHOU De-rui. Combined corrosion inhibitors for secondary alkaline zinc electrodes[J]. Battery Bimonthly, 2004, 34(2): 111-113.

[14] CAO Chu-nan, ZHANG Jian-qing. Introduction to Electrochemical Impedance Spectroscopy[M]. Beijing: Science Press, 2002. 169-170.

[15] SHEN De-yan. Application of IR Spectroscopy in Research of Macromolecules[M]. Beijing: Science Press, 1982. 55-56.

(Edited by LONG Huai-zhong)